Available online at www.sciencedirect.com
SCIENCE DIRECT
International Journal of Heat and Mass Transfer 49 (2006) 2227–2238
International Journal of HEAT and MASS TRANSFER
www.elsevier.com/locate/ijhmt

Improved formulation of electron kinetic theory approach for laser ultra-short-pulse heating

Bekir Sami Yilbas *

Department of Mechanical Engineering and Minerals, King Fahd University of Petroleum and Minerals, P.O. Box 1913, Dhahran 31261, Saudi Arabia

Received 8 December 2004; received in revised form 19 September 2005
Available online 20 February 2006

Abstract

The formulation of energy transport in electron and lattice sub-systems due to the laser ultra-short-pulse heating of metallic surface is carried out using an electron kinetic theory model. The rate of electron energy gain from the irradiated field and its dissipation through the collisional process are taken into account in the analysis. The constant and variable physical properties are introduced in the numerical simulations. The two-equation and electron kinetic theory models formulated previously are also employed for the comparison purposes. It is found that the improved electron kinetic theory formulation predicts relatively lower lattice site temperatures as compared to the two-equation and electron kinetic theory models formulated previously. The results of the improved formulation is similar to that obtained for the hyperbolic heating model.

Keywords: Laser; Heating; Short-pulse; Energy; Transport

1. Introduction

During the laser heating of the metallic substrates, electrons within the absorption depth of the substrate material gain energy from the irradiated field through the absorption process. This, in turn, increases the electron energy and results in transferring of their excess energy to lattice site through scattering, which depends upon the duration of the interaction. In the case of short-pulses (slightly higher than the electron–phonon interaction time), electrons undergo few collisions with lattice site, since the electron–phonon collision time is in the order of 0.02 ps [1]. Moreover, electrons in the surface region continuously gain energy from the irradiated field, which in turn results in energy differences between the electrons and the lattice site in this region. The specific heat capacity of electron is much smaller than its counterpart corresponding to the lattice site; consequently, electron temperature increases rapidly while lattice site temperature increase is gradual during the short heating duration. The temperature differential between electron and lattice sub-systems results in non-equilibrium energy transport in the substrate material. However, energy distribution of the excited electrons may not be uniform in the surface region and also varies with time. This causes temperature differential occurring in the electron sub-system. Consequently, when modelling the heating process, the non-equilibrium energy transport and time variation effect of the energy transport from electron to lattice sub-systems should be accommodated in the analysis.

Considerable research studies were carried out to explore the laser short pulse heating of solid surfaces. Anisimov et al. [2] investigated the effect of intense light fluxes on metals. They introduced the electronic thermal conductivity in the model. Laser ultra-short pulse interaction with metals was studied by Agranat et al. [3]. They indicated that above certain laser power intensities, temperature of the electron sub-system was detached from that of

* Tel.: +966 3 860 2540; fax: +966 3 860 2949.
E-mail address: bsyilbas@kfupm.edu.sa

0017-9310/$ - see front matter © 2006 Elsevier Ltd. All rights reserved.
doi:10.1016/j.ijheatmasstransfer.2005.10.047

Nomenclature

A	$A = \frac{fk\tau_s}{\lambda^2}$
B	$(B = k)$ where k is thermal conductivity (W/m K)
C	$C = \frac{fk}{\lambda^2}\left(1 - \frac{fk\tau_s}{\rho Cp\lambda^2}\right)$
D	$D = \rho Cp - \frac{fk\tau_s}{\lambda^2}$
ABS	absolute value
C_e	electron heat capacity (J/m^3 K)
C_l	lattice heat capacity (J/m^3 K)
Cp	specific heat of lattice site (J/kg K)
ΔE	energy transferred to lattice site (J)
f	fraction of excess energy exchange
G	electron phonon coupling factor (W/m^3 K)
I_0	laser peak power intensity (W/m^2)
J	total energy carried by a laser pulse divided by the laser spot cross section (J/m^2)
k	thermal conductivity (W/m K)
k_B	Boltzmann's constant (1.38×10^{-23} J/K)
m_e	electron mass (kg)
N	electron number density (1/m^3)
r_f	reflection coefficient
S	source term
T_l	lattice site temperature (K)
T_e	electron temperature (K)
T_d	Debye temperature (K)
t	time (s)
t_p	FWHM duration of the laser pulse (s)
Δt	time increment (s)
$\overline{V}$	electron mean velocity (m/s)
s	spatial coordinates corresponding to the electron movement (m)
x	spatial coordinates corresponding to the x-axis for phonon (m)
Δx	spatial increment (m)
α	thermal diffusivity (m^2/s)
δ	absorption coefficient (1/m)
λ	mean free path of electrons (m)
ρ	density (kg/m^3)
τ_p	electron mean free time between electron–phonon coupling (s)
τ_s	electron–phonon characteristic time $\left(\tau_s = \frac{C_e}{G}\right)$ (s)

ion sub-system. A non-local macroscopic formulation of heat transport due to steep temperature gradients was considered by Luciani and Mora [4]. They indicated that the expression derived for the heat flux described fairly well the heat transport in a steep temperature gradient. Fujimoto et al. [5] investigated non-equilibrium temperatures in electron and lattice sub-systems during the femtosecond laser heating of metallic tungsten. They showed from pump-probe measurements that a transient non-equilibrium temperature difference between electron and lattice sub-systems occurred and the electron–phonon energy relaxation time of several hundred femtoseconds resulted. The generation of non-equilibrium electron and lattice temperatures in copper by picosecond laser pulses was investigated by Eesley [1]. He indicated that the measurement results agreed well with the model based on separation of the one-dimensional heat flow equation into electron and lattice sub-systems. Thermal relaxation of electrons in metals was formulated by Allen [6]. He developed a simple expression for the thermal relaxation rate. The femtosecond pump-probe measurements of the electron–phonon coupling constant within films of metals and components were carried out by Brorson et al. [7]. They indicated that the measurement results agreed well with the theoretical predictions. The hyperbolic heat conduction due to a mode locked laser pulses was studied by Hector et al. [8]. They showed that the differences between the hyperbolic and parabolic model became less extreme as the pulse frequency decreased. The comparative studies on non-linear hyperbolic and parabolic heat conduction for various boundary conditions were considered by Kar et al. [9]. They indicated that as time progresses, the results of the hyperbolic and parabolic conduction became identical due to the relaxation term, which became unimportant for large heating periods. Heat transfer mechanisms during laser short-pulse heating of metals was studied by Qiu and Tien [10]. They showed that the solution of the Boltzmann equation leaded to a hyperbolic heat flux equation for electrons. A relaxation model for heat conduction and generation was examined by Malinowski [11]. He indicated that the relaxation solution did not tend to converge the corresponding parabolic solution. The time-resolved electron temperature measurement in a highly excited gold target was carried out by Wang et al. [12]. They indicated that both electron–phonon and electron–electron scattering contributed to the electron relaxation rate. A universal constitutive equation between the heat flux vector and the temperature gradient was proposed by Tzou [13]. He showed that the universal form of the energy equation facilitated identifications of the physical parameters governing the transition from one mechanism to another such as diffusion or wave to electron–phonon interaction. The non-equilibrium laser heating of metal films was investigated by Al-Nimr and Al-Masoud [14]. They simplified the governing equations and introduced an analytical solution to the heating problem. The unsteady solution of a unified heat conduction equation was presented by Lin et al. [15]. They discussed the applicability of the solution presented. A formulation of hyperbolic heat conduction based on a scalar field was proposed by Barletta and Zanchini [16]. They indicated that the proposed formulation of the heating problem was especially useful when step changes (in time evolution

of either the boundary temperature or the boundary heat flux occurred) were presented. The ballistic approach for heat conduction equations based on Boltzmann equation was presented by Chen [17]. He showed that the ballistic equations developed were a better approximation than the Fourier law and Cattaneo equation for heat conduction at the scales when the device characteristic length was comparable to the heat-carrier mean free path and/or characteristic time was comparable to the heat-carrier relaxation time. Voisin et al. [18] were discussed the femtosecond optical response of noble metal nanoparticles and its connection to the ultra-fast electron dynamics in the light of the results of high-sensitivity femtosecond pump-probe experiment. The findings were compared to the ones in the bulk materials. Electron kinetic theory approach was introduced by Yilbas [19] when modeling the laser heating process. The governing equations of energy transport was based on the collisional process that takes place between the excited electrons and the phonons. Yilbas and Shuja [20] showed that the predictions of the electron kinetic theory approach, the two equation model, and the Fourier heating model became identical for the heating periods greater than sub-nanoseconds. The comparison of one and three-dimensional energy transport due to a laser heating pulse was studied by Yilbas [21]. He indicated that temperature profiles obtained from one and three-dimensional models were almost identical during the early heating period (shorter than the thermalization time). In this case, the time variation of electron excess energy transfer to lattice sub-system becomes important during the short heating period.

The hyperbolic model for laser short-pulse heating process was introduced using the Boltzmann's equations [10,17]. Moreover, the electron kinetic theory approach can also be used to model the non-equilibrium energy transport and time variation effect of the energy transport from electron to lattice sub-systems. In the present study, ultra-short laser pulse heating of copper is considered and the energy transport due to a ultra-short laser heating pulse is formulated using an electron kinetic theory approach. The effect of ultra-short heating duration on the energy absorption and its transportation in the electron and lattice sub-systems is accommodated in the analysis.

2. Mathematical analysis of heating process

The mathematical arrangements of the two-equation model and electron kinetic theory approach are presented briefly, since the details of the analyses can be found elsewhere [1,22,23].

2.1. Two-equation model

The two-equation model representing the energy exchange mechanism during phonon absorption and electron–phonon coupling after one-dimensional consideration can be written as [1]:

$$C_e\frac{\partial T_e(s,t)}{\partial t} = \nabla\cdot(k\nabla T_e(s,t)) - G[T_e(s,t) - T_l(x,t)] + S$$
$$C_l\frac{\partial T_l(x,t)}{\partial t} = G[T_e(s,t) - T_l(x,t)] \quad (1)$$

$T_e(s,t)$ and $T_l(x,t)$ are the electron and lattice site temperatures, S is the laser source term ($I_0\delta\exp(-\delta x)$), and C_e and C_l are the electron and lattice heat capacities, respectively. G is the electron–phonon coupling factor, given by [24]:

$$G = \frac{\pi^2 m_e N \overline{V}^2}{6\tau_p T_e(s,t)} \quad (2)$$

where m_e, N, $\overline{V}$, and τ_p are electron mass, electron number density, electron drift velocity, and the electron–phonon collision time, respectively.

2.2. Electron kinetic theory approach

In order to formulate the electron kinetic theory approach for the laser short-pulse heating process, the investigation into the electron motion in the surface region of the metallic substrates is necessary. The electron motion in the surface region of the metals due to the irradiated field can be shown schematically in Fig. 1. Electrons travel from surface to solid bulk as well as bulk to solid. Electrons reaching the surface can escape once their energy exceeds the surface potential barrier. Consequently, the number of electrons with ψ fraction reaching the surface can manage to escape. In order to account for the reflected electrons from the surface, a mirror image at the surface is considered [19]. Consider the location A in Fig. 1, the net flow of N_{sx} ($\sim\frac{N}{6}$) number of electrons towards the surface occurs and ψ fraction of these electrons may escape from the surface. The situation, which occurs at location A in Fig. 1 is an exact mirror image of that corresponding to point B, i.e. $(1-\psi)N_{sx}$ number electrons still flow towards the surface from location B, i.e. $(1-\psi)N_{sx}$ electrons flow to the right and $\frac{N}{6}$ to the left at location B (Fig. 1). In the case of location A approaches to location B, the number

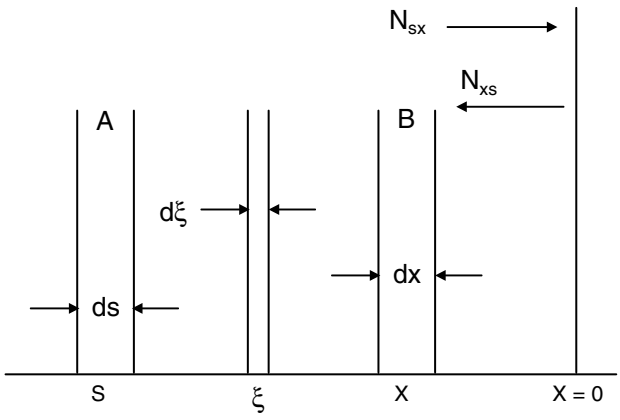

Fig. 1. Electron movement in the surface region ($x = 0$ is the free surface).

of electrons N_{sx}, which flow from "s" to "x" changes discontinuously at $s=0$ and at $s=x$. These changes can be summarized as follows:

In the negative direction of x

$$\begin{aligned} -\infty < s < x &: N_{xs} = \frac{N}{6} \\ x < s < 0 &: N_{xs} = (1-\psi)\frac{N}{6} \\ 0 < s < \infty &: N_{xs} = \frac{N}{6} \end{aligned} \tag{3}$$

and

In the positive direction of x

$$\begin{aligned} -\infty < s < 0 &: N_{sx} = \frac{N}{6} \\ 0 < s < x &: N_{sx} = (1-\psi)\frac{N}{6} \\ x < s < \infty &: N_{sx} = \frac{N}{6} \end{aligned} \tag{4}$$

Moreover, at all locations:

$$N_{sx} + N_{xs} = (2-\psi)\frac{N}{6}$$

where N_{xs} is the number of electrons, which flow from "x" to "s".

It should be noted that changes in N_{sx} follows a distribution, which can be described by a rectangle function of unit height and width "x" centered on the positive $s=\frac{x}{2}$. Consequently, the rectangle function can be written as

$$\prod \frac{(s-\frac{x}{2})}{x} = \prod \frac{(2s-x)}{2x} \tag{5}$$

where

$$\prod \frac{(2s-x)}{2x} = 0 \quad \text{for } |2s-x| > \frac{1}{2}$$

and

$$\prod \frac{(2s-x)}{2x} = 1 \quad \text{for } |2s-x| < [x| \tag{6}$$

Therefore, the electron distribution can be described as

$$N_{sx} = \frac{N}{6}\left(1-\psi\prod\frac{(2s-x)}{2x}\right)$$
$$\text{with } N_{sx}+N_{xs} = (1-\psi)\frac{N}{6} \tag{7}$$

It should be noted that electron energy, which is characterized by temperature $T_e(s,t)$, is augmented from the initial $T_e(s,t)$ by an amount equal to that absorbed in travelling from s to x. The total amount of energy, which is absorbed in an element $\mathrm{d}\xi$, area A in time δt is

$$I_0 A\,\mathrm{d}t\,\mathrm{d}\xi f'(\xi) \tag{8}$$

where I_0 and $f'(\xi)$ are the laser peak power intensity and the intensity distribution function in the absorption depth of the solid material, since all the beam energy is absorbed in the x-axis. The electron density can vary along the x-axis, in particular, the number of electrons travelling from $\mathrm{d}s$ to $\mathrm{d}x$ may not be the same as that from $\mathrm{d}x$ to $\mathrm{d}s$. Therefore, the portion of energy which is absorbed by electrons which travel from $\mathrm{d}s$ to $\mathrm{d}x$ in $\mathrm{d}t$ is

$$I_0 A\,\mathrm{d}t f'(\xi)\,\mathrm{d}\xi\frac{N_{sx}}{N_{sx}+N_{xs}} \tag{9}$$

where N_{sx} and N_{xs} are the number of electrons which travel from s to x and from x to s, respectively. The total number of electrons which travel from $\mathrm{d}s$ to $\mathrm{d}x$ in this time is

$$N_{sx}A\overline{V}\,\mathrm{d}t \tag{10}$$

where $\overline{V}$ is electron mean velocity. Hence, the average energy absorbed by one electron in $d\xi$ in time $\mathrm{d}t$ is

$$I_0\frac{f'(\xi)\,\mathrm{d}\xi}{(N_{sx}+N_{xs})\overline{V}} \tag{11}$$

and the total amount of energy absorbed by this electron from $\mathrm{d}x$ to $\mathrm{d}s$ is

$$\int_x^s I_0\frac{f'(\xi)\,\mathrm{d}\xi}{(N_{sx}+N_{xs})\overline{V}} \tag{12}$$

This expression gives the extra energy gain by the electrons in travelling from $\mathrm{d}s$ to $\mathrm{d}x$.

Electrons receive energy from the irradiated field and make collisions among them selves as well as lattice site ions and they transfer some fraction of their excess energy through the collisional process, i.e. electrons after the first collision scatter and make further collisions with less energetic electrons and lattice site ions. The energy exchange between energetic electrons, due to absorption of the irradiated field, and other species can be formulated after considering the collision probability of energetic electrons.

Consider the probability of electrons travelling a distance "x" without making a collision is [25]:

$$\exp\left(-\frac{x}{\lambda}\right)$$

where $x < 2\lambda$ and λ is the mean free path of the electrons. Consider Fig. 1, the probability of electrons, which make collision in B can be written as

$$1-\exp\left(-\frac{x}{\lambda}\right)$$

or

$$1-\left(1-\frac{\mathrm{d}x}{\lambda}+\cdots\right)$$

or

$$\sim\frac{\mathrm{d}x}{\lambda}$$

provided that $x < 2\lambda$. The probability of electrons which last collided in B now colliding in A is

$$\frac{\mathrm{d}s}{\lambda}\exp\left(-\frac{|x-s|}{\lambda}\right)\frac{\mathrm{d}x}{\lambda}$$

However, the number of electrons (N_{sx}) leaving the location A in Fig. 1, area A in time $\mathrm{d}t$ is

$$N_{sx}A\overline{V}\,\mathrm{d}t$$

where N_{sx} is the number density of electrons which transfer energy from $\mathrm{d}x$ to $\mathrm{d}s$, and $\overline{V}$ is the mean electron velocity. The number these electrons which have just collided in location A is

$$N_{sx}A\overline{V}\,\mathrm{d}t\frac{\mathrm{d}s}{\lambda}\frac{\mathrm{d}x}{\lambda}\exp\left(-\frac{|x-s|}{\lambda}\right)$$

where $\frac{\mathrm{d}s}{\lambda}\frac{\mathrm{d}x}{\lambda}\exp\left(-\frac{|x-s|}{\lambda}\right)$ is the probability of electrons just collided in location A.

If the temperature of lattice site in $\mathrm{d}x$ is $T_\mathrm{l}(x,t)$ and the temperature of the electrons when they arrive at $\mathrm{d}x$ is $T_\mathrm{e}(s,t)$ (allowing for absorption on the way), then the energy transfer to the lattice site in $\mathrm{d}x$ from collisions with electrons in which the electrons give up a fraction "f" of their excess energy is

$$N_{sx}A\overline{V}\,\mathrm{d}t\frac{\mathrm{d}s}{\lambda}\frac{\mathrm{d}x}{\lambda}\exp\left(-\frac{|x-s|}{\lambda}\right)f(E_\mathrm{e}-E_\mathrm{l})$$

where E_e and E_l are the energy of electron and lattice ion, respectively. The analysis related to f is given in Appendix A. Integrating the contributions from all such infinitely small strips as to the energy in location B (Fig. 1) gives:

$$\int_{-\infty}^{\infty}N_{sx}A\overline{V}\,\mathrm{d}t\frac{\mathrm{d}s}{\lambda}\frac{\mathrm{d}x}{\lambda}\exp\left(-\frac{|x-s|}{\lambda}\right)f(E_\mathrm{e}-E_\mathrm{l})\,\mathrm{d}s \tag{13}$$

In this case, energy transfer during Δt ($\Delta t \geqslant \tau_\mathrm{p}$, where τ_p is the electron–phonon collision time) due to absorption of irradiated field and the collisional process can be written after incorporating electron distribution function (Eq. (7)) [22]:

$$\begin{aligned}\frac{\Delta E_\mathrm{trans}}{A\,\mathrm{d}x\Delta t} &= \int_{-\infty}^{\infty}\frac{\overline{V}fk_\mathrm{B}}{\lambda^2}N_{sx}\left(1-\psi\prod\frac{(2s-x)}{2x}\right)\\ &\times\exp\left(-\frac{|x-s|}{\lambda}\right)T_\mathrm{e}(s,t)\,\mathrm{d}s\\ &-\int_{-\infty}^{\infty}\frac{\overline{V}fk_\mathrm{B}}{\lambda^2}N_{sx}\left(1-\psi\prod\frac{(2s-x)}{2x}\right)\\ &\times\exp\left(-\frac{|x-s|}{\lambda}\right)T_\mathrm{l}(x,t)\,\mathrm{d}s\\ &+\int_{-\infty}^{\infty}\frac{I_0 f}{\lambda^2}\frac{N_{sx}}{N_{sx}+N_{xs}}\\ &\times\exp\left(-\frac{|x-s|}{\lambda}\right)\int_x^s f'(\xi)\,\mathrm{d}\xi\,\mathrm{d}s\end{aligned} \tag{14}$$

where

$$\frac{N_{sx}}{N_{sx}+N_{xs}}=\frac{\left(1-\psi\prod\frac{(2s-x)}{x}\right)}{2-\psi}$$

where f is the fraction of electron excess energy, which transfers to lattice site during a single electron lattice site collision. The first term on the left hand side of Eq. (14) is energy gain by the substrate material through the collisional process, first and second terms on the right hand side represent electron and lattice energies, and third therm on the right hand site is the energy gain of the electrons due to the irradiated field.

The final temperature of the electrons in $\mathrm{d}x$ after the collisional process can be readily found from the conservation of energy, i.e.

Total electron energy after collision

= Total electron energy in during $\mathrm{d}t$

− Change of lattice site energy

Total electron energy after collision is

$$\begin{aligned}&\int_{-\infty}^{\infty}\frac{\overline{V}k_\mathrm{B}}{\lambda^2}N_{sx}\left(1-\psi\prod\frac{(2s-x)}{2x}\right)\\ &\times\exp\left(-\frac{|x-s|}{\lambda}\right)(T_\mathrm{e}(s,t)-fT_\mathrm{l}(x,t))\,\mathrm{d}s\end{aligned} \tag{15}$$

Total electron energy carried into $\mathrm{d}x$ during $\mathrm{d}t$ is

$$\begin{aligned}&\int_{-\infty}^{\infty}\frac{\overline{V}k_\mathrm{B}(1-f)}{\lambda^2}N_{sx}\left(1-\psi\prod\frac{(2s-x)}{2x}\right)\\ &\times\exp\left(-\frac{|x-s|}{\lambda}\right)T_\mathrm{e}(s,t)\,\mathrm{d}s\\ &+\int_{-\infty}^{\infty}\frac{I_0(1-f)}{\lambda^2}\frac{\left(1-\psi\prod\frac{(2s-x)}{2x}\right)}{2-\psi}\\ &\times\exp\left(-\frac{|x-s|}{\lambda}\right)\int_x^s f'(\xi)\,\mathrm{d}\xi\,\mathrm{d}s\end{aligned} \tag{16}$$

Therefore, the conservation of energy yields:

$$\begin{aligned}&\int_{-\infty}^{\infty}\frac{\overline{V}k_\mathrm{B}}{\lambda^2}N_{sx}\left(1-\psi\prod\frac{(2s-x)}{2x}\right)\exp\left(-\frac{|x-s|}{\lambda}\right)\\ &\times(T_\mathrm{e}(s,t)-fT_\mathrm{l}(x,t))\,\mathrm{d}s\\ &=\int_{-\infty}^{\infty}\frac{\overline{V}k_\mathrm{B}(1-f)}{\lambda^2}N_{sx}\left(1-\psi\prod\frac{(2s-x)}{2x}\right)\\ &\times\exp\left(-\frac{|x-s|}{\lambda}\right)T_\mathrm{e}(s,t)\,\mathrm{d}s\\ &+\int_{-\infty}^{\infty}\frac{I_0(1-f)}{\lambda^2}\frac{\left(1-\psi\prod\frac{(2s-x)}{2x}\right)}{2-\psi}\\ &\times\exp\left(-\frac{|x-s|}{\lambda}\right)\int_x^s f'(\xi)\,\mathrm{d}\xi\,\mathrm{d}s\end{aligned} \tag{17}$$

Eqs. (14) and (17) can be re-written after considering the electron distributions (Eq. (7)) for the lattice element $\mathrm{d}x$ apart and for electrons passing an area A, i.e.

$$\begin{aligned}\frac{\Delta E_{\text{trans}}}{A\,\mathrm{d}x\Delta t} &= \int_{-\infty}^{\infty}\frac{fk}{\lambda^3}\exp\left(-\frac{|x-s|}{\lambda}\right)T_{\mathrm{e}}(s,t)\,\mathrm{d}s \\ &- \int_{-\infty}^{\infty}\frac{fk}{\lambda^3}\exp\left(-\frac{|x-s|}{\lambda}\right)T_1(x,t)\,\mathrm{d}s \\ &+ \int_{0}^{|x|}\psi\frac{fk}{\lambda^3}\exp\left(-\frac{|x-s|}{\lambda}\right)T_1(x,t)\,\mathrm{d}s \\ &- \int_{0}^{|x|}\psi\frac{fk}{\lambda^3}\exp\left(-\frac{|x-s|}{\lambda}\right)T_{\mathrm{e}}(s,t)\,\mathrm{d}s \\ &+ \int_{-\infty}^{\infty}\frac{I_0 f}{\lambda^2}\frac{1}{(2-\psi)}\exp\left(-\frac{|x-s|}{\lambda}\right)\int_x^s f'(\xi)\,\mathrm{d}\xi\,\mathrm{d}s \\ &- \int_{-\infty}^{\infty}\frac{I_0 f}{\lambda^2}\frac{\psi}{(2-\psi)}\exp\left(-\frac{|x-s|}{\lambda}\right)\int_x^s f'(\xi)\,\mathrm{d}\xi\,\mathrm{d}s \end{aligned} \tag{18}$$

and

$$\begin{aligned}&\int_{-\infty}^{\infty}\frac{k}{\lambda^2}\exp\left(-\frac{|x-s|}{\lambda}\right)(T_{\mathrm{e}}(s,t)-fT_1(x,t))\,\mathrm{d}s \\ &- \int_{0}^{|x|}\frac{\psi k}{\lambda^2}\exp\left(-\frac{|x-s|}{\lambda}\right)(T_{\mathrm{e}}(s,t)-fT_1(x,t))\,\mathrm{d}s \\ &= \int_{-\infty}^{\infty}\frac{k(1-f)}{\lambda^2}\exp\left(-\frac{|x-s|}{\lambda}\right)T_{\mathrm{e}}(s,t)\,\mathrm{d}s \\ &- \int_{0}^{|x|}\frac{k(1-f)}{\lambda^2}\exp\left(-\frac{|x-s|}{\lambda}\right)T_{\mathrm{e}}(s,t)\,\mathrm{d}s \\ &+ \int_{-\infty}^{\infty}\frac{I_0(1-f)}{\lambda^2(2-\psi)}\exp\left(-\frac{|x-s|}{\lambda}\right)\int_x^s f'(\xi)\,\mathrm{d}\xi\,\mathrm{d}s \\ &- \int_{0}^{|x|}\frac{I_0(1-f)}{\lambda^2(2-\psi)}\exp\left(-\frac{|x-s|}{\lambda}\right)\int_x^s f'(\xi)\,\mathrm{d}\xi\,\mathrm{d}s \end{aligned} \tag{19}$$

where k is the thermal conductivity, which makes use of the simple kinetic theory result for the electron thermal conductivity [26]:

$$k = \frac{N\overline{V}k_{\mathrm{B}}\lambda}{3} \tag{20}$$

The energy content of the small lattice site element $\mathrm{d}x$ apart can be written as

$$\Delta E = A\,\mathrm{d}xC_1T_1(x,t) \tag{21}$$

where $C_1 = \rho Cp$. The energy gain of the small lattice element during the small time interval δt is $\frac{\Delta E}{\delta t}$. The expansion of $\frac{\Delta E}{\delta t}$ yields:

$$\frac{\Delta E}{\delta t} = \frac{1}{\delta t}\left[E(t)+\delta tE'(t)+\frac{(\delta t)^2}{2!}E''(t)+\cdots-E(t)\right] \tag{22}$$

or

$$\frac{\Delta E}{\delta t} = E'(t)+\frac{(\delta t)}{2!}E''(t)+\cdots \tag{23}$$

Combining Eqs. (21) and (23) yield:

$$\frac{\Delta E}{\delta t} = A\,\mathrm{d}x\left\{C_1\frac{\partial}{\partial t}[T_1(x,t)]+C_1\frac{(\delta t)}{2!}\frac{\partial^2}{\partial t^2}[T_1(x,t)]+\cdots\right\} \tag{24}$$

When the time increment approaches to thermal relaxation time ($\delta t \to \tau_{\mathrm{s}}$), Eq. (24) reduces to

$$\frac{\partial e}{\partial t} = \frac{\Delta E}{\delta t A\,\mathrm{d}x} \simeq C_1\frac{\partial}{\partial t}[T_1(x,t)+\tau_{\mathrm{s}}\frac{\partial}{\partial t}(T_1(x,t))] \tag{25}$$

where e is the volumetric energy content of lattice site. The energy gain of the small lattice element through collisional energy transport can also be written as

$$\frac{\Delta E}{A\,\mathrm{d}x\Delta t} = \frac{1}{A\,\mathrm{d}x}\left[\frac{\Delta E_{\text{trans}}}{\Delta t}+\tau_{\mathrm{s}}\frac{\partial}{\partial t}\left(\frac{\Delta E_{\text{trans}}}{\Delta t}\right)\right] \tag{26}$$

Substituting Eq. (18) into Eq. (26) yields and the change of lattice site energy is

$$\begin{aligned}\frac{\Delta E}{A\delta x\Delta t} =& \left\{\begin{array}{l}\displaystyle\int_{-\infty}^{\infty}\frac{fk}{\lambda^3}\exp\left(-\frac{|x-s|}{\lambda}\right)T_{\mathrm{e}}(s,t)\,\mathrm{d}s-\int_{-\infty}^{\infty}\frac{fk}{\lambda^3}\exp\left(-\frac{|x-s|}{\lambda}\right)T_1(x,t)\,\mathrm{d}s \\ \displaystyle+\int_{0}^{|x|}\psi\frac{fk}{\lambda^3}\exp\left(-\frac{|x-s|}{\lambda}\right)T_1(x,t)\,\mathrm{d}s-\int_{0}^{|x|}\psi\frac{fk}{\lambda^3}\exp\left(-\frac{|x-s|}{\lambda}\right)T_{\mathrm{e}}(s,t)\,\mathrm{d}s \\ \displaystyle+\int_{-\infty}^{\infty}\frac{I_0 f}{\lambda^2}\frac{1}{(2-\psi)}\exp\left(-\frac{|x-s|}{\lambda}\right)\int_x^s f'(\xi)\,\mathrm{d}\xi\,\mathrm{d}s \\ \displaystyle-\int_{-\infty}^{\infty}\frac{I_0 f}{\lambda^2}\frac{\psi}{(2-\psi)}\exp\left(-\frac{|x-s|}{\lambda}\right)\int_x^s f'(\xi)\,\mathrm{d}\xi\,\mathrm{d}s\end{array}\right\} \\ &+\tau_{\mathrm{s}}\frac{\partial}{\partial t}\left\{\begin{array}{l}\displaystyle\int_{-\infty}^{\infty}\frac{fk}{\lambda^3}\exp\left(-\frac{|x-s|}{\lambda}\right)T_{\mathrm{e}}(s,t)\,\mathrm{d}s-\int_{-\infty}^{\infty}\frac{fk}{\lambda^3}\exp\left(-\frac{|x-s|}{\lambda}\right)T_1(x,t)\,\mathrm{d}s \\ \displaystyle+\int_{0}^{|x|}\psi\frac{fk}{\lambda^3}\exp\left(-\frac{|x-s|}{\lambda}\right)T_1(x,t)\,\mathrm{d}s-\int_{0}^{|x|}\psi\frac{fk}{\lambda^3}\exp\left(-\frac{|x-s|}{\lambda}\right)T_{\mathrm{e}}(s,t)\,\mathrm{d}s \\ \displaystyle+\int_{-\infty}^{\infty}\frac{I_0 f}{\lambda^2}\frac{1}{(2-\psi)}\exp\left(-\frac{|x-s|}{\lambda}\right)\int_x^s f'(\xi)\,\mathrm{d}\xi\,\mathrm{d}s \\ \displaystyle-\int_{-\infty}^{\infty}\frac{I_0 f}{\lambda^2}\frac{\psi}{(2-\psi)}\exp\left(-\frac{|x-s|}{\lambda}\right)\int_x^s f'(\xi)\,\mathrm{d}\xi\,\mathrm{d}s\end{array}\right\}\end{aligned} \tag{27}$$

Eqs. (19) and (27) are the energy transport equations of interest for laser short pulse heating process. However, for small rise of electron temperature during the low intensity laser heating pulse prevents electron escape from the surface. Consequently, the term ψ in Eqs. (19) and (27) becomes zero.

Eqs. (19) and (27) can be transformed into differential equations. The method of solution to be used in the following analysis is the transformation of the simultaneous differential–integral equations (19) and (27) using the Fourier integral transformation, with respect to x [22]. This is due to the fact that the resultant ordinary differential equations may then be handled much more conveniently. Consider first reduction of the set of equations to the differential equation of heat conduction.

The Fourier transformation of a function $f(x)$ is defined by

$$F[f(x)] = \int_{-\infty}^{\infty}\exp(-\mathrm{i}\omega x)f(x)\,\mathrm{d}x = F(\omega) \tag{28}$$

and the Fourier inversion by

$$f(x) = \frac{1}{2\pi}\int_{-\infty}^{\infty}F(\omega)(\exp(-\mathrm{i}\omega x)\,\mathrm{d}\omega \tag{29}$$

The Fourier transformation of the convolution integral:

$$\int_{-\infty}^{\infty}f(\xi)g(x-s)\,\mathrm{d}s \tag{30}$$

is the produces of the transforms:

$$\bar{f}(\omega)\cdot\bar{g}(\omega) \tag{31}$$

and the transform of function $\exp\left(-\frac{|x|}{\lambda}\right)$ is

$$\frac{2\lambda}{1+\omega^2\lambda^2} \tag{32}$$

Therefore, the Fourier transform of the function:

$$IX = \int_{-\infty}^{\infty} \frac{k}{\lambda^3} \exp\left(-\frac{|x-s|}{\lambda}\right) T_l(x,t)\,\mathrm{d}s \tag{33}$$

will be a constant factor (the value of integral) multiplying the transform of the function $T_l(x,t)$, i.e.

$$F[IX] = \frac{kf}{\lambda^3}\overline{T_l}F\left\{\int_{-\infty}^{\infty} \exp\left(-\frac{|x-s|}{\lambda}\right)\mathrm{d}s\right\} \tag{34}$$

or

$$F[IX] = \frac{kf}{\lambda^3}\overline{T_l}F\left\{\int_{-\infty}^{\infty} \exp\left(-\frac{|x-s|}{\lambda}\right)H(|s|)\,\mathrm{d}s\right\} \tag{35}$$

where $H(|s|) = 1$ for $-\infty < s < \infty$.

Therefore

$$\begin{aligned} F[IX] &= \frac{kf}{\lambda^3}\overline{T_l}F\left\{\int_{-\infty}^{\infty} \exp\left(-\frac{|x-s|}{\lambda}\right)\right\}F\{H(|s|)\,\mathrm{d}s\} \\ &\leqslant \frac{kf}{\lambda^3}\overline{T_l}\frac{2\lambda}{\omega^2\lambda^2+1}\delta(\omega) \end{aligned} \tag{36}$$

where $\delta(\omega)$ is the Dirac delta function. Since this function only has a value of 1 at $\omega = 0$, then the transform is

$$\frac{kf}{\lambda^2}\overline{T_l} \tag{37}$$

Using these results, the Eqs. (19) and (27) can be Fourier transformed, the result of which is

$$\begin{aligned} \frac{\overline{\partial e}}{\partial t} &= \frac{kf}{\lambda^3}\left[\frac{2\lambda}{\omega^2\lambda^2+1}\overline{T_e}\right] - \frac{kf}{\lambda^2}\overline{T_l} \\ &\quad + \left[\frac{I_0\delta f}{2\lambda}\right]\left[\frac{2\lambda}{\omega^2\lambda^2+1}\right]\left[\frac{2\delta}{\delta^2+\omega^2}\right]\tau_p \\ &\quad \times \frac{\partial}{\partial t}\left[\frac{kf}{\lambda^3}\left[\frac{2\lambda}{\omega^2\lambda^2+1}\overline{T_e}\right]\right] - \frac{kf}{\lambda^2}\overline{T_l} \\ &\quad + \left[\frac{I_0\delta f}{2\lambda}\right]\left[\frac{2\lambda}{\omega^2\lambda^2+1}\right]\left[\frac{2\delta}{\delta^2+\omega^2}\right] \end{aligned} \tag{38}$$

and

$$\begin{aligned} \frac{k}{\lambda^2}[\overline{T_e} - f\overline{T_l}] &= \left[\frac{k(1-f)}{\lambda^3}\right]\left[\frac{2\lambda}{\omega^2\lambda^2+1}\right]\overline{T_e} \\ &\quad + \frac{I_0\delta(1-f)}{2\lambda}\left[\frac{2\lambda}{\omega^2\lambda^2+1}\right]\left[\frac{2\delta}{\delta^2+\omega^2}\right] \end{aligned} \tag{39}$$

If the transform function $\overline{T_e}$ is obtained from Eq. (39) using Eq. (38), the result is

$$\begin{aligned} [f+\omega^2\lambda^2]\frac{\overline{\partial e}}{\partial t} &= -\omega^2 kf\overline{T_l} - \tau_p\frac{\partial}{\partial t}(\omega^2 kf\overline{T_l}) \\ &\quad + I_0\delta f\left[\frac{2\delta}{\delta^2+\omega^2}\right] + \tau_p\frac{\partial}{\partial t}\left[I_0\delta f\left[\frac{2\delta}{\delta^2+\omega^2}\right]\right] \end{aligned} \tag{40}$$

Insertion of $\frac{\partial e}{\partial t}$ in terms of T_l (Eq. (25)) and multiplication of Eq. (40), which is in the transform domain, by $(\mathrm{i}\omega)^2$ corresponds to second order differential in the real plane. Hence the inversion of the above equation gives:

$$\begin{aligned} &\left[\left(1+\tau_s\frac{\partial}{\partial t}\right) - \frac{\lambda^2}{f}\frac{\partial^2}{\partial x^2}\right]C_l\frac{\partial T_l}{\partial t} \\ &\quad = k\frac{\partial^2 T_l}{\mathrm{d}x^2} + \tau_p\frac{\partial}{\partial t}\left(\frac{\partial^2 T_l}{\mathrm{d}x^2}\right) + I_0\delta f\exp(-\delta|x|) \\ &\qquad + \tau_p\frac{\partial}{\partial t}[I_0\delta f\exp(-\delta|x|)] \end{aligned} \tag{41}$$

Eq. (41) is similar to that obtained from the ballistic approach [17]. It should be noted that the time derivative of diffusion $\left(\tau_p\frac{\partial}{\partial t}\left(\frac{\partial^2 T_l}{\mathrm{d}x^2}\right)\right)$ and source $\left(\frac{\partial}{\partial t}[I_0\delta f\exp(-\delta|x|)]\right)$ terms are included in Eq. (41) as similar to the that obtained from the ballistic approach [17].

2.2.1. Parabolic heating model

If the terms $\tau_p\frac{\partial}{\partial t}\left(\frac{\partial^2 T_l}{\mathrm{d}x^2}\right)$ and $\tau_p\frac{\partial}{\partial t}[I_0\delta f\exp(-\delta|x|)]$ are neglected in Eq. (41) for all f values, Eq. (41) becomes:

$$\left[\left(1+\tau_s\frac{\partial}{\partial t}\right) - \frac{\lambda^2}{f}\frac{\partial^2}{\partial x^2}\right]C_l\frac{\partial T_l}{\partial t} = k\frac{\partial^2 T_l}{\mathrm{d}x^2} + I_0\delta f\exp(-\delta|x|) \tag{42}$$

which is the same as previously formulated kinetic theory model [23], i.e. the time derivative of diffusion and source terms are omitted in the previously formulated kinetic theory approach. Eq. (42) can be re-written as

$$\begin{aligned} C_l\frac{\partial T_l}{\partial t} &= k\frac{\partial^2 T_l}{\mathrm{d}x^2} + f\frac{\lambda^2\partial^2}{\partial x^2}\left(\rho Cp\frac{\partial T_l}{\partial t}\right) - C_l\tau_s\frac{\partial^2 T_l}{\partial t^2} \\ &\quad + I_0\delta\exp(-\delta|x|) \end{aligned} \tag{43}$$

Eq. (43) is a third order partial differential equation, which can be decomposed into second and first order two differential equations, i.e., when Eq. (43) is decomposed into two equations, the resulting probable differential equations are

$$\begin{aligned} A\frac{\partial T_e}{\partial t} &= B\frac{\partial^2 T_e}{\mathrm{d}x^2} - C[T_e - T_l] + I_0\delta\exp(-\delta|x|) \\ D\frac{\partial T_l}{\partial t} &= C[T_e - T_l] \end{aligned} \tag{44}$$

where A, B, C, and D are the coefficients. To find the values of A, B, C, and D, the following procedure is adopted, i.e.

$$D\frac{\partial^2 T_l}{\partial t^2} = C\left[\frac{\partial T_e}{\partial t} - \frac{\partial T_l}{\partial t}\right] \tag{45}$$

or

$$\frac{\partial T_e}{\partial t} = \frac{D}{C}\frac{\partial^2 T_l}{\partial t^2} + \frac{\partial T_l}{\partial t} \tag{46}$$

Similarly

$$D\frac{\partial^2}{\partial x^2}\left(\frac{\partial T_l}{\partial t}\right)=C\left[\frac{\partial^2 T_e}{\partial x^2}-\frac{\partial^2 T_l}{\partial x^2}\right] \tag{47}$$

or

$$\frac{\partial^2 T_e}{\partial x^2}=\frac{D}{C}\frac{\partial^2}{\partial x^2}\left(\frac{\partial T_l}{\partial t}\right)+\frac{\partial^2 T_l}{\partial x^2} \tag{48}$$

Substitution of Eqs. (46) and (48) into Eq. (44), and inserting $C[T_e - T_l] = D\frac{\partial T_l}{\partial t}$ into Eq. (44), it yields:

$$(D+A)\frac{\partial T_l}{\partial t}=\frac{BD}{C}\frac{\partial^2}{\partial x^2}\left(\frac{\partial T_l}{\partial t}\right)+B\frac{\partial^2 T_l}{\partial x^2}-\frac{AD}{C}\frac{\partial^2 T_l}{\partial t^2}+I_0\delta\exp(-\delta|x|) \tag{49}$$

After equating Eqs. (43) and (49), the coefficients A, B, C, and D can be calculated, i.e.

$$\begin{aligned}A&=\frac{fk\tau_s}{\lambda^2}\\ B&=k\\ C&=\frac{fk}{\lambda^2}\left(1-\frac{fk\tau_s}{\rho Cp\lambda^2}\right)\\ D&=\rho Cp-\frac{fk\tau_s}{\lambda^2}\end{aligned} \tag{50}$$

Eq. (44) is identical to Eq. (1) given in the two-equation model. Consequently, setting the coefficients of Eqs. (44) and (1), it yields:

$$\begin{aligned}&\frac{fk\tau_s}{\lambda^2}=C_e\\ &\frac{fk}{\lambda^2}\left(1-\frac{fk\tau_s}{\rho Cp\lambda^2}\right)=G\\ &\rho Cp-\frac{fk\tau_s}{\lambda^2}=C_l\end{aligned} \tag{51}$$

where $\tau_s = C_e/G$ [10] and $C_e = \gamma T_e$ (where γ is constant and $\gamma = 96.6\ \mathrm{J/m^3\ K^2}$ for copper). Moreover, the electron phonon coupling factor is temperature dependent, which can be written as [24]:

$$G=\frac{\pi^2 mN\overline{V}^2}{6\tau_p(T_e)T_e} \tag{52}$$

Eq. (52) can be used for lattice site temperature less than the Debye temperature (343 K for copper). Since the electron–phonon collision time $\tau_p \sim \frac{1}{T_e}$, the electron phonon coupling factor becomes constant as temperature increases [5,27], i.e. it becomes independent of temperature.

The electron mean free path (λ) can be written as [28]:

$$\lambda=\overline{V}\tau \tag{53}$$

where τ is the electron relaxation time, which is [29]:

$$\tau=\frac{3mk}{\pi^2 Nk_B^2 T_e}$$

where N and m are electron number density and effective mass of free electrons, respectively. k_B is the Boltzmann's constant. The electron mean free path can be determined from Eq. (53). The range of mean free path determined is given in Table 1.

2.2.2. Initial and boundary conditions

To solve Eq. (41), the following initial and boundary conditions are employed.

Initially (before the initiation of the laser pulse) the lattice and electron sub-systems are considered at the same initial temperature (T_0), i.e.

At time $t = 0 \rightarrow T_l = T_0$ and $T_e = T_0$

The substrate material surface is considered to be insulated (no convective and radiative heat losses from the surface), i.e.

At the surface at $x = 0 \rightarrow \frac{\partial T_l}{\partial x} = 0$ and $\frac{\partial T_e}{\partial x} = 0$

The substrate material is considered to extend at considerable depth from the surface; in which case, electron and lattice temperatures attain equilibrium at temperature T_0, i.e.

At far depth from the free surface x
$= 20 \times \delta(\delta$ being absorption depth)
$\rightarrow T_l = T_0$ and $T_e = T_0$

2.3. Numerical solution

The numerical method employed uses a explicit finite difference scheme, which is well established in the literature [30]. Although similar arguments are presented in the previous study [23], in order to secure the completeness of the arguments the stability criteria is introduced herein. The stability criteria for the heating model is as follows:

$$\begin{aligned}1 \geqslant\ &\mathrm{ABS}\left[\frac{fC_l}{\Delta t}+2\lambda^2 C_l\left[\frac{1}{\Delta t(\Delta x)^2}\right]-2kf\left[\frac{1}{(\Delta x)^2}\right]\right]\\ &+\mathrm{ABS}\left[\frac{kf}{(\Delta x)^2}-\frac{2\lambda^2 C_l}{\Delta t(\Delta x)^2}\right]+\mathrm{ABS}\left[\frac{2\lambda^2 C_l}{\Delta t(\Delta x)^2}\right]\\ &-\mathrm{ABS}\left\{\frac{fC_l}{\Delta t}+2\lambda^2 C_l\left[\frac{1}{\Delta t(\Delta x)^2}\right]\right\}\end{aligned} \tag{54}$$

Table 1
Thermal properties of copper at 300 K [1]

T_d (K)	γ (J/m^3 K^2)	$\delta\times10^7$ (1/m)	$m\times10^{-31}$ (kg)	$C_l\times10^6$ (J/K m^3)	k (W/m K)	$G\times10^{16}$ (W/m^3 K)	τ_s (ps)	τ_p (ps)	$N\times10^{28}$ (1/m^{-3})	$\overline{V}$ (m/s)
343	96.6	7.1	9.1	3.43	386	26	0.1562	0.024	8.4	5010

Table 2
The coefficients and the range of values used in the simulations

λ (m)	f	$A\times10^4$ (W/m^3 K)	B (W/m K)	$C\times10^{16}$ (W/m^3 K)	$D\times10^6$ (J/m^3 K)	$I_0(1-r_f)$ (W/m^2)
10^{-9}–5×10^{-10}	10^{-3}–10^{-5}	2.52–2.09	386	24–28	3.27–3.49	0.5×10^{12}

where Δx is spatial increments in the x axis while Δt is the time increment.

The step input laser pulse with power intensity 0.5×10^{12} W/m^2 is considered in the simulations. It is assumed that the laser wavelength is in the visible spectrum (630). Thermophysical properties of copper at 300 K and laser pulse properties used in the computations are given in Tables 1 and 2.

2.4. Validation of numerical prediction

To validate the present predictions, the transient reflectivity data given in the previous study [31] are considered. It should be noted that in the early heating period, the lattice temperature change is considerably small and the surface reflectivity change is due to electron temperature rise in this period. In this case, the reflectivity change can be related with the electron temperature change [32], i.e.

$$\frac{\Delta R}{(\Delta R)_{\max}}=\frac{\Delta T_e}{(\Delta T_e)_{\max}}$$

In order to proceed with the comparison, the experimental condition including the laser pulse used in the experiment is employed in the simulations [30]. In the previous experiment, the laser source was a colliding-pulse mode-locked (CPM) dye laser with a wavelength 630 nm [30]. The laser source term, for the validation simulations, is

$$0.94\frac{1-R}{t_p}\delta J\exp\left(-x\delta-2.77\left(\frac{t}{t_p}\right)^2\right)$$

where t_p is full-width-at-half-maximum (FWHM) duration of the laser pulse, and $t=0$ is defined at the moment when the peak of a laser pulse arrives at the metal surface. J is the total energy carried by a laser pulse divided by the laser spot cross section. In the validation simulations, $t_p=96$ fs and $J=10$ J/m^2 are employed.

Fig. 2 shows the temporal variation of the normalized reflectivity change obtained from the experiment and predicted from two equation as well as improved electron kinetic theory approach for gold film. It is evident that the improved electron kinetic theory approach and two equation model predict similar normalized reflectivity. Moreover, the results obtained from the improved electron kinetic theory approach give slightly closer results to experimental data as compared to that corresponding to the two-equation model, particularly for time period less than 1 ps.

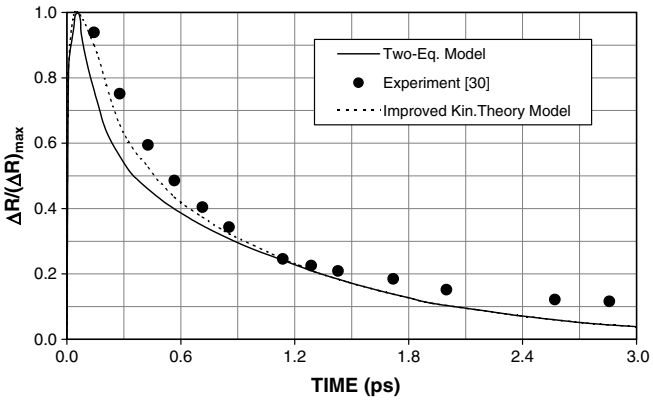

Fig. 2. Temporal variation of normalized reflectivity change obtained from the previous study [30], two-equation model, and improved electron kinetic theory approach.

3. Results and discussion

Laser short pulse heating of copper is modelled using an electron kinetic theory approach. Since the behavior of the electron movement in the early heating period results in non-equilibrium energy transport in the electron sub-system, the formulation of the heating problem allowing the rate of electron excess energy gain and dissipation in this period is considered. The improved formulation of the electron kinetic theory approach accounts for the rate of electron excess energy gain and dissipation in the early heating period different than those corresponding the previously developed electron kinetic theory approach and the two equation model. This, in turn, gives the realistic electron–phonon coupling mechanism in the heating model similar to that presented in the ballistic approach [17]. Moreover, the two-equation and the kinetic theory models for the parabolic heating case are also presented for the comparison purposes. The variable and constant physical properties are introduced in the numerical simulations.

Fig. 3 shows lattice site temperature obtained from different heating models for constant and variable properties for two heating periods. The variable properties case predicts slightly higher lattice site temperatures in the surface region than that corresponding to the constant properties case. This is because of the electron–phonon coupling factor (G), which does not vary considerably with changing electron temperature (Eq. (52)). The similar situation is also observed in the previous study [30]. Moreover, the two-equation and the parabolic electron kinetic theory models predict almost identical temperature profiles for the constant and variable properties cases. This may be explained in terms of Eqs. (1) and (44) and their coeffi-

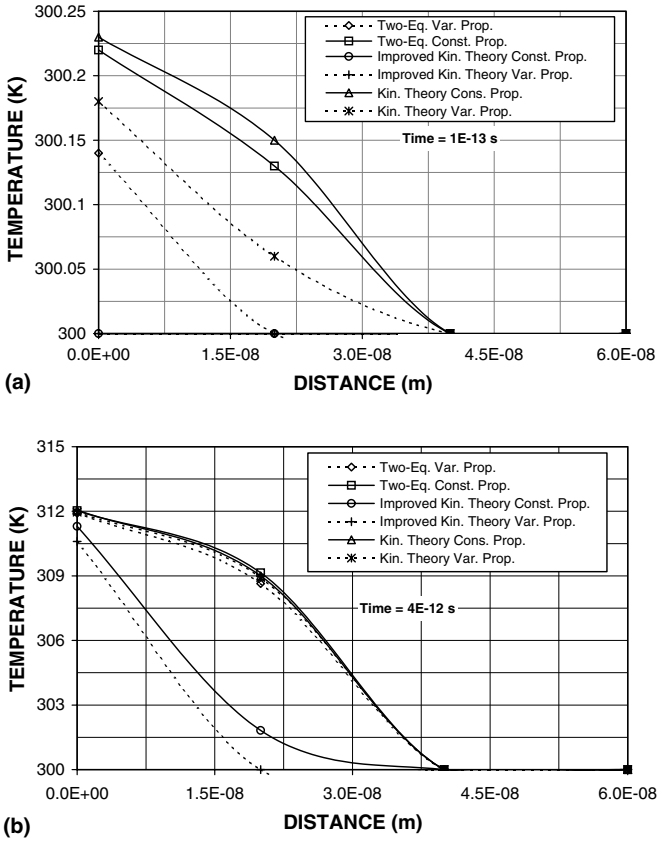

Fig. 3. Lattice site temperature distribution inside copper for (a) 1×10^{-13} s and (b) 4×10^{-12} s heating period.

cients, i.e. Eq. (1) representing the two-equation model and coefficients of the differential terms are almost identical to Eq. (44), which corresponds to the previously formulated electron kinetic theory approach. In the case of improved kinetic theory formulation, lattice site temperature is less than those corresponding to other models employed. This indicates that in the early heating period, electrons absorbing energy from the irradiated field do not transfer all their excess energy to lattice site through collisional process. This occurs because of the few number of collisions, which take place in the early heating period, i.e. excess electron energy transferring to lattice site is considerably less in the early heating period. The improved electron kinetic theory approach results in realistic electron–phonon coupling between the electrons and the lattice site in the early heating period, which is particularly true in the surface vicinity of the substrate material. This can be observed from Fig. 2; in which case, the experimental results for reflectivity change agree well with the improved electron kinetic theory predictions. It should be noted that Fig. 2 is plotted for gold film [31], i.e. the experiment was carried out for gold substrate; consequently, simulations were repeated for gold substrate due to comparison.

Fig. 4 shows temporal variation of lattice site temperature at the surface as obtained from the different models with constant and variable properties cases. In general,

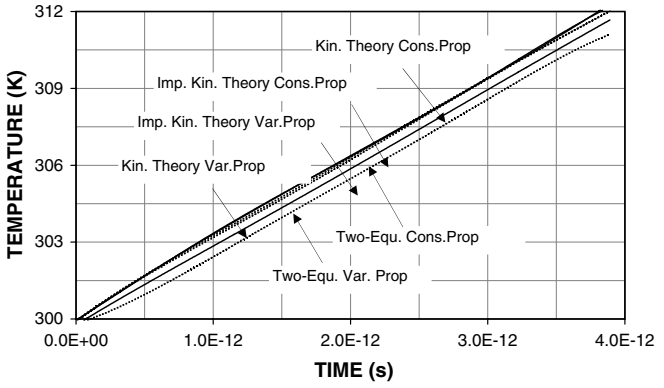

Fig. 4. Temporal variation of lattice site temperature distribution at the surface.

temporal variations of lattice site temperature due to different models and properties are similar, provided that some small differences in temperature profiles occur. The similar behavior of temperature profiles is because of the magnitude of temperature rise, which is in the order of 12 °C. In the early heating period, the rise of lattice site temperature is considerably small, which is particularly true for improved kinetic theory model. In the early heating period ($t < 10^{-13}$ s) electrons undergo few collisions, since the time for an electron–phonon collision is in the order of 0.02 ps [1], i.e. lattice site heating by electrons through collisional process is not possible for times less than the collision time. Moreover, improved electron kinetic theory formulation allows non-equilibrium energy transport in the electron and lattice sub-systems. Consequently, the rate of lattice site temperature rise in the early heating period differs than that corresponding to parabolic formulation of the electron kinetic theory and the two-equation models. This situation occurs for the constant as well as variable properties cases. It should be noted that constant and variable properties cases represent the results obtained from the simulations due to constant and variable properties being employed in the governing equation, respectively. In this case, electron excess energy increases due to the absorption of the irradiated field and the coupling between the electron and lattice site is considerable small, electron temperature rises rapidly while lattice site temperature rise is gradual in the early heating period. This behavior is also observed for the situation occurring in the hyperbolic two-equation model [10]. The term $\tau_p \frac{\partial}{\partial t}\left(\frac{\partial^2 T_l}{dx^2}\right)$ in Eq. (41) suppresses lattice site temperature rise in the early heating period. The parabolic formulation of electron kinetic theory predictions agreed well with the two-equation model (parabolic heating model). Moreover improved electron kinetic theory formulation with constant properties case results in excessive delaying of the rise of lattice site temperature, i.e. the delay is in the order of 1.2×10^{-13} s. However, in the case of variable properties case, this delay is in the order of 6×10^{-14} s, which is more realistic than the constant properties case due to few number of collisions taking place during this time period.

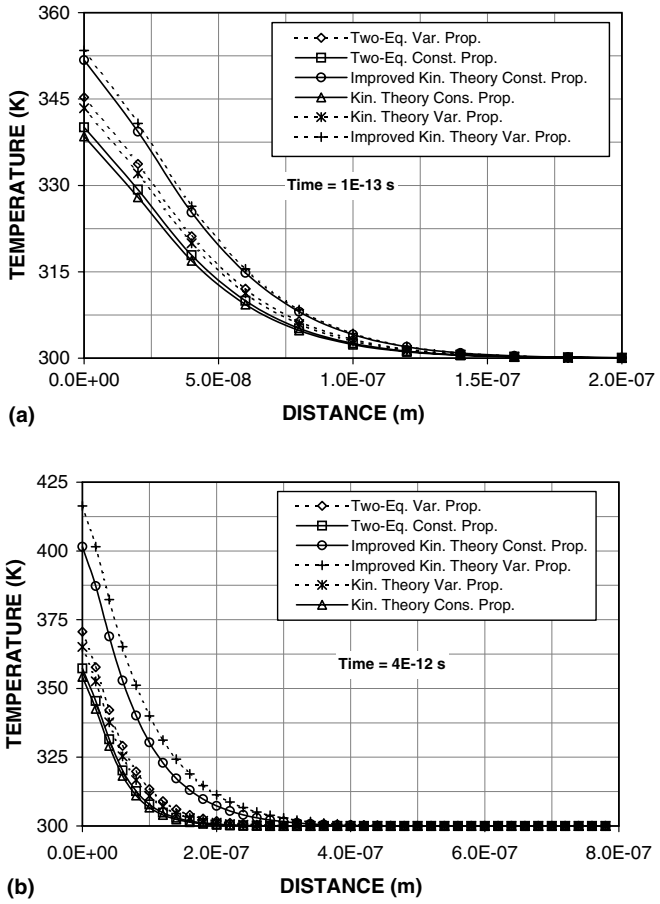

Fig. 5. Electron temperature distribution inside copper for (a) 10^{-13} s and (b) 4×10^{-12} s heating period.

Fig. 5 shows electron temperature distribution inside the surface region of the substrate material for two heating periods. Electron temperature decays gradually in the surface vicinity while it decays sharply in the region next to the surface vicinity. This is because of the absorption of the irradiated energy, which decays exponentially with increasing depth from the surface (Lambert's law). In the early heating period, electron temperature profiles corresponding to all models employed are similar provided that constant properties case results in relatively low temperature magnitudes. As the heating period increases to 4×10^{-12} s, temperature distributions corresponding to different models vary considerably. This occurs because of the collisional energy transport process, in which case, electron excess energy transfers to lattice site at different rates. It should be noted that specific heat capacity of electrons is lower than lattice site specific heat capacity ($Cp_e/Cp_l\approx10^{-2}$), large amount of electron excess energy transfer to lattice site results in substantial change in electron temperature while lattice site temperature increase is small. This situation can be seen when comparing Figs. 3 and 5. In the case of improved electron kinetic theory formulation, the term $\left(\tau_p\frac{\partial}{\partial t}\left(\frac{\partial^2 T_l}{dx^2}\right)\right)$ in Eq. (41) further suppresses the electron excess energy transfer to lattice site. This results in high electron and low lattice site temperatures in the region irradiated by the laser beam.

4. Conclusions

Laser short-pulse heating of copper is considered. The two-equation heating model and parabolic formulated electron kinetic theory approach, and improved electron kinetic theory formulation are introduced when modelling the non-equilibrium energy transport in the electron and lattice sub-systems. In order to account for the influence of temperature dependent properties on the predictions, constant and variable physical properties are introduced in the analysis. A numerical method is employed to solve the governing equations of energy transport. It is found that in the early heating period (10^{-13} s), all the models employed predict almost identical electron temperature distribution inside the substrate material. This occurs because of electrons, which undergo few collisions with lattice site during the early heating period. Consequently, the amount of electron excess energy gain and dissipation, due to absorption of the irradiated field and collisional process, becomes almost the same for all the models. As the heating period progresses (4×10^{-12} s), the amount of energy transport from electrons to lattice site through the collisional process is governed by the electron–phonon coupling process. In this case, the two-equation model and previously formulated electron kinetic theory approach result in early rise of lattice site temperature. In the case of improved electron kinetic theory formulation, the term $\left(\tau_p\frac{\partial}{\partial t}\left(\frac{\partial^2 T_l}{dx^2}\right)\right)$ in Eq. (41) suppresses the lattice site temperature rise, particularly in the early heating period. Consequently, improved formulation of electron kinetic theory model predicts low lattice site temperature rise as similar to that corresponding to the hyperbolic and ballistic heating models. The two-equation model (parabolic heating model) predictions agreed well with the previously formulated electron kinetic theory model.

Acknowledgement

The author acknowledge the support of King Fahd University of Petroleum and Minerals, Dhahran, Saudi Arabia, for this work.

Appendix A. Formulation of f

The fraction of electron excess energy transfer during the time comparable or slightly greater than the electron–phonon collision time (τ_p) can be written in terms of the energy balance across the section dx in the substrate material, i.e.

$$f=\frac{(\text{Electron energy})_{in}-(\text{Electron energy})_{out}}{(\text{Electron energy})_{in}-(\text{Phonon energy})}$$

or

$$f = \frac{(T_e)_{in} - (T_e)_{out}}{(T_e)_{in} - T_l} \tag{55}$$

where $(T_e)_{in}$ is the temperature of an electron entering the section, $(T_e)_{out}$ temperature of the an electron leaving the section, and T_l is the phonon temperature. f takes the values $0 \leqslant f \leqslant 1$.

References

[1] G.L. Eesley, Generation of nonequilibrium electron and lattice temperatures in copper by picosecond laser pulses, Phys. Rev. B 33 (1986) 2144–2151.

[2] S.I. Anisimov, A.M. Bonch-Bruevich, M.A. El'yashevich, Y.A. Imas, N.A. Pavlenko, G.S. Romanov, Effect of powerful light fluxes on metals, Sov. Phys. Techn. Phys. 11 (1967) 945–952.

[3] M.B. Agranat, A.A. Benditskii, G.M. Gandel'man, A.G. Devyatkov, P.S. Kondratenko, B.I. Makshantsev, G.I. Rukman, B.M. Stepanov, Noninertial radiation from metals in interaction with ultra-short pulses of coherent infrared radiation, JETP Lett. 30 (1979) 167–169.

[4] J.F. Luciani, P. Mora, J. Virmont, Nonlocal heat transport due to steep temperature gradients, Phys. Rev. Lett. 51 (1983) 1664–1667.

[5] J.G. Fujimoto, J.M. Liu, E.P. Ippen, Femtosecond laser interaction with metallic tungsten and nonequilibrium electron and lattice temperatures, Phys. Rev. Lett. 53 (1984) 1837–1840.

[6] P.B. Allen, Theory of thermal relaxation of electrons in metals, Phys. Rev. Lett. 59 (1987) 1460–1463.

[7] S.D. Brorson, A. Kazeroonian, J.S. Moodera, D.W. Face, T.K. Cheng, E.P. Ippen, M.S. Dresselhaus, G. Dresselhaus, Femtosecond room-temperature measurement of the electron–phonon coupling constant λ in metallic superconductors, Phys. Rev. Lett. 64 (1990) 2172–2175.

[8] L.G. Hector Jr., W.S. Kim, M.N. Ozisik, Hyperbolic heat conduction due to mode locked laser pulse train, Int. J. Eng. Sci. 30 (1992) 1731–1744.

[9] A. Kar, C.L. Chan, J. Mazumder, Comparative studies on nonlinear hyperbolic heat conduction for various boundary conditions: analytical and numerical solutions, ASME J. Heat Transfer 114 (1992) 14–20.

[10] T.Q. Qiu, C.L. Tien, Heat transfer mechanisms during short-pulse laser heating of metals, ASME J. Heat Transfer 115 (1993) 835–841.

[11] L. Malinowski, A relaxation model for heat conduction and generation, J. Phys. D: Appl. Phys. 26 (1993) 1176–1180.

[12] X.Y. Wang, D.M. Riffe, Y.S. Lee, M.C. Downer, Time-resolved electron-temperature measurement in a highly excited gold target using femtosecond thermionic emission, Phys. Rev. B 50 (1994) 8016–8019.

[13] D.Y. Tzou, A unified field approach for heat conduction from macro-to-micro-scales, ASME J. of Heat Transfer 117 (1995) 8–16.

[14] M.A. Al-Nimr, S.A. Masoud, Nonequilibrium laser heating of metal films, ASME J. Heat Transfer 119 (1997) 188–190.

[15] C. Lin, C. Hwang, Y. Chang, The unsteady solutions of a unified heat conduction equation, Int. J. Heat Mass Transfer 40 (1997) 1716–1719.

[16] A. Barletta, E. Zanchini, A thermal potential formulation of hyperbolic heat conduction, ASME J. Heat Transfer 121 (1999) 166–169.

[17] G. Chen, Ballistic-diffusive heat-conduction equations, Phys. Rev. Lett. 86 (2001) 2297–2300.

[18] C. Voisin, N. Del Fatti, D. Christofilos, F. Vallee, Ultrafast electron dynamics and optical nonlinearities in metal nanoparticles, J. Phys. Chem., Part B 105 (12) (2001) 2264–2280.

[19] B.S. Yilbas, Heating of metals at a free surface by laser radiation an electron kinetic theory approach, Int. J. Eng. Sci. 24 (8) (1986) 1325–1334.

[20] B.S. Yilbas, S.Z. Shuja, Laser short-pulse heating of surfaces, J. Phys. D: Appl. Phys. 32 (1999) 1947–1954.

[21] B.S. Yilbas, Electron kinetic theory approach—one-and three-dimensional heating with pulsed laser, Int. Heat Mass Transfer 44 (2001) 1925–1936.

[22] B.S. Yilbas, A.Z. Sahin, An approach to convergency of kinetic theory to Fourier theory in relation to laser heating process, Jpn. J. Appl. Phys. 32 (Part 1, 12A) (1993) 5646–5651.

[23] B.S. Yilbas, A.F.M. Arif, Material response to thermal loading due to short pulse laser heating, Int. J. Heat Mass Transfer. 44 (2001) 3787–3798.

[24] M.I. Kaganov, I.M. Lifshiftz, L.V. Tanatarov, Relaxation between electrons and crystalline lattice, Sov. Phys. JETP 4 (1957) 173–178.

[25] L.B. Loeb, The Kinetic Theory of Gases, Dover, NY, 1961.

[26] C.L. Tien, J.H. Lienhard, Statistical Thermodynamics, Hemisphere, Washington, DC, 1979.

[27] H.E. Elsayed-Ali, M.A. Norris, M.A. Pessot, G.A. Mourou, Time-resolved observation of electron–phonon relaxation in copper, Phys. Rev. Lett. 58 (1987) 1212–1215.

[28] M. Honner, J. Kunes, On the wave diffusion and parallel nonequilibrium heat conduction, ASME J. Heat Transfer 121 (1999) 702–707.

[29] T.Q. Qiu, L. Tien, Femtosecond laser heating of multi-layer metals-I analysis, Int. J. Heat Mass Transfer 37 (1994) 2789–2797.

[30] G.D. Smith, Numerical Solution of Partial Differential Equations Finite Difference Methods, third ed., Clarendon Press, Oxford, 1985.

[31] S.D. Brorson, J.G. Fujimoto, E.P. Ippen, Femtosecond electron heat-transport dynamics in thin gold film, Phys. Rev. Lett. 59 (1987) 1962–1965.

[32] D.Y. Tzou, K.S. Chiu, Temperature-dependent thermal lagging in ultrafast laser heating, Int. J. Heat Mass Transfer 44 (2001) 1725–1734.